Detection of Micro Contamination in Hard Disk Drives using Maximum Likelihood Estimation and Angle Detection

Jirarat Ieamsaard*[1] and Paisarn Muneesawang[1]
[1]Department of Electrical and Computer Engineering, Faculty of Engineering, Naresuan University, Phitsanulok, Thailand
*jirarati55@email.nu.ac.th, paisarnmu@nu.ac.th

Frode Eika Sandnes[2,3]
[2]Instzitute of information Technology, Faculty of Technology, Art and Design, Oslo and Akershus University College of Applied Sciences, Oslo
[3]Westerdals Oslo School of Art, Communication and Technology, Oslo, Norway
Frode-Eika.Sandnes@hioa.no

Abstract— **Micro contamination is one of the critical defects that occur on the head gimbal assembly (HGA). The HGA is a key component of the read/write assembly of a hard disk drive. This paper presents an image-based automatic inspection method for micro-contamination detection. Maximum likelihood estimation combined with angle measurements are proposed for identifying defects. The performance of the proposed maximum likelihood estimation and angle measurement method is compared to previous angle measurement and intensity thresholding methods. The experimental results show that the fusion of maximum likelihood estimation and angle measurements outperforms the angle measurement and intensity thresholding method with an accuracy of 87.9 % compared the accuracy of 80.1% reported in previous work.**

Keywords-component; micro contamination; maximum likelihood estimation; angle measurement

I. INTRODUCTION (HEADING 1)

Hard disk drives (HDDs) are the primary storage devices used in computers and consumer electronic devices. The demand for storage is constantly growing. Although users are increasingly storing their information in the cloud, the cloud services still relies on physical storage. To meet the increasing storage demands hard disk manufacturers need to constantly improve their technology and manufacturing processes. One important phase of HDD manufacturing is the inspection of HDD components. Several challenges arise due to the miniaturization of HDDs and their components.

This study focuses on the inspection of the Air bearing surface (ABS) of the Head gimbal assembly (HGA) which is the key read/write component of a HDD. In the manufacturing plant discussed herein, the inspection of HGAs is performed by a visual inspection machine. Images automatically captured by a set of cameras are automatically inspected using the commercial COGNEX image analysis system. This automatic inspection system has a low accuracy and results in a high false detection rate. This study thus proposes a new method to improve the performance of automatic contamination detection.

978-1-5090-2033-1/16/$31.00 ©2016

II. PREVIOUS WORK

There have been several experimental studies on the automatic visual inspection of hard disk defects such as the detection of defects on the HDD media surface using spectral imaging [1], [2]. Withayachumnankul et al. [3] devised a filter kernel to detect the edges of hairline crack defects on the surface of piezoelectric actuators. Yammen et al. [4] explored the inspection of corrosions on pole tips at the end of an air-bearing slider using area-based and contour-based features. In another image-based attempt [5] three steps were explored to identify contamination on the ABS. First, the input image was preprocessed to segment ABS sub-image from the original top-view image of the HGA. Next, potential contamination areas were identified using circle detection in up-sampled ABS images. Finally, each of the contamination contenders were classified as being either a contamination or not by using angle measurements and an intensity threshold. The method proposed in [5] does not rely on template images. However, the angle measurement and intensity threshold caused many false detections with the low quality of the test images that were used. For that reason, this study proposes an improved method that attempts to reduce the false detection rate.

III. THE PROPOSED METHOD

The proposed method starts with a preprocessing step to locate the ABS region in the HGA image. Then, circle detection is used to locate potential contamination areas. Cross-covariance, likelihood, and angle measurement are used to determine whether a potential contamination area is actually contaminated or not. The details of the approach are described in the following sections.

A. *Preprocessing*

In this study RGB input images of HGAs with a resolution of 2400×2000 pixels (96 dpi) were used. It was assumed that the camera capturing the HGA top view was stationary relative to the units on the conveyer belt. Normalized cross correlation [4, 6] was employed to determine the region of interest relative to an ABS template image. A sub-image representing a 490×414 pixel region of interest is extracted and converted to grayscale. The grayscale sub-image is registered with an ABS template image using intensity-based registration [7]. The

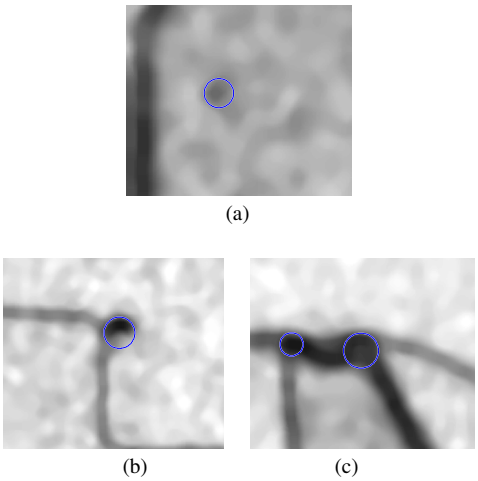

(a)

(b) (c)

Figure 1. Example of circle detection; a)-b) contamination circles, (c) non-contamination circle.

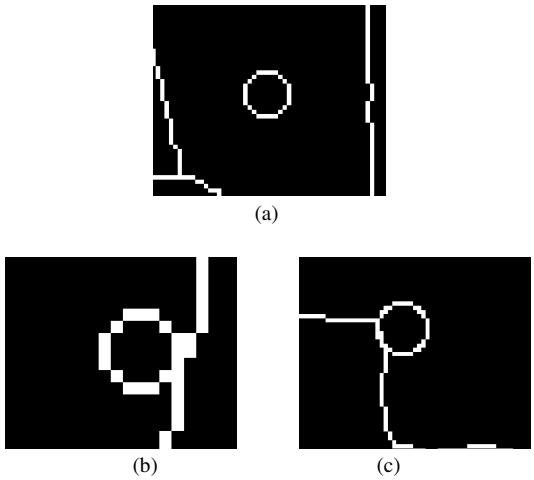

(a)

(b) (c)

Figure 2. Circles detected in the skeleton image; a) number of cross-points = 0, b) number of cross-points =1, and c) number of cross-points ≥2.

grayscale ABS images are up-sampled [8] by a factor of five, since some contaminations are small. Up-sampled images are anti-aliased using a 15×15 median filter [9]. A circle Hough transforms is used to determine potential areas of contamination in the up-sampled image. Circle centers and radii are transformed back to the coordinate system of the original image.

B. *Determine crosspoint*

Next, the detected circles are classified as a contamination or non-contamination using the cross-point, cross-covariance feature [10], maximum likelihood estimate and angle measurement.

To locate cross-points, the skeleton of the template is used. A grayscale version of the ABS template image is low-pass filtered and high pass filtered. The difference between the low pass-filtered image and high pass-filtered image is then binarized using Otsu's method [11]. Otsu's method employs adaptive thresholding for image segmentation, where the local threshold is computed from the variance within each class. The

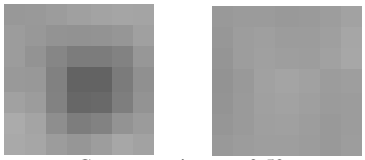

Cross-covariance = 0.53

(a)

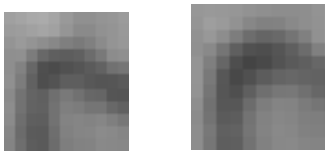

Cross-covariance = 0.11

(b)

Figure 3. Example of square region; a) contamination square region, and b) non-contamination square region.

morphological skeleton operator is subsequently applied to the binarized image of the template image to obtain a skeleton of the ABS binary image. The circles detected in the previous step are traced on the skeleton image with a 50% larger radii ($radius_{new} = (6/4) \cdot radius_{old}$) to find points where the circumference of the detected circles crosses the skeleton [5]. Each circle is considered according to three cases depending on the number of cross-point on each circle; case:1 is number of cross-points = 0, case:2 is number of cross-points =1, and case:3 is number of cross-points ≥2.

C. *Cross-covariance feature*

Square region of the grayscale test image and the grayscale template image are detected using the circle centers and radii found during the preprocessing step.

To estimate the similarity of the test image and the template image their cross covariance [10] is computed.

D. *Likelihood Estimation*

Several researchers have employed the maximum likelihood function in their work [12, 13, 14]. In this study, we classify input images by using likelihood function of the cross-covariance features. Let x be the cross-covariance feature vector. Also, let $P(x|w_i)$ be the likelihood of class w_i, where w_1 is the contamination class and w_2 is the non-contamination class. In order to determine the likelihood function: $P(x|w_1)$ *and* $P(x|w_2)$, in the experiment section, cross-covariance features were collected from training data set, which covers 427 contamination squares of 313 contaminated ABS images and 23,721 non-contamination squares of 500 uncontaminated ABS images. The likelihood function was obtained using the histogram [16].

After finding the cross-points each circle it is assigned one of three cases. A separate likelihood function is considered for each case.

Case 1 – no cross-points: The detected circle is not present on the ABS template skeleton. The likelihood of the contamination class and the non-contamination class are computed from the probability density of the cross-covariance feature of the training data.

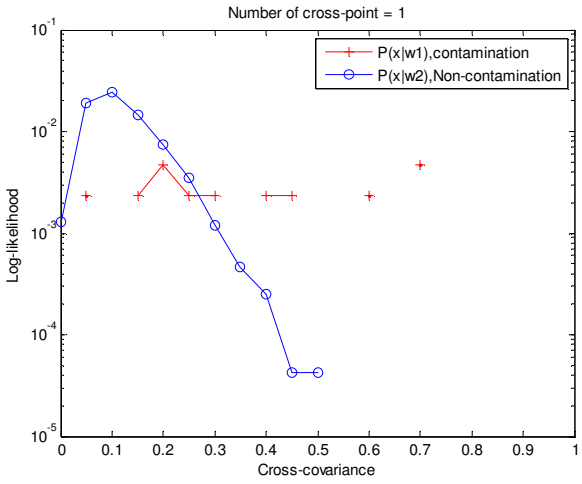

Figure 4. Log-likelihood function for case 2

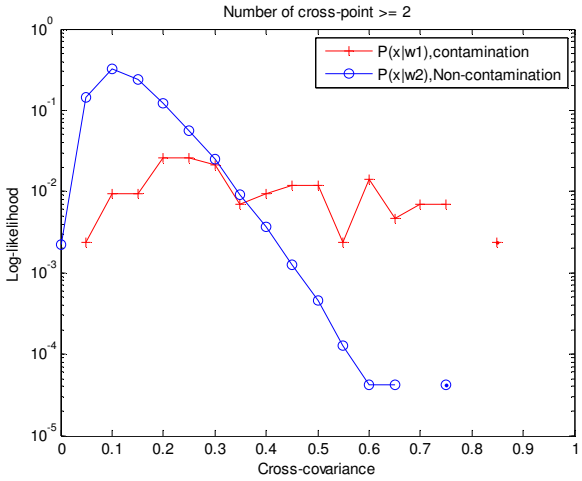

Figure 5. Log-likelihood function for case 3

Case 2 – one cross-point: There is one pixel of the circumference of the detected circle intersects with the skeleton. The likelihood of the contamination class and the non-contamination class are obtained from the cross-covariance of the training data. Figure 4 shows the log-likelihood $P(x|w_1)$ of class w_1 (contamination) and the log-likelihood $P(x|w_2)$ of class w_2 (non-contamination).

Case 3 – more than one cross-point: There is at least two pixels of the circumference of the detected circle that intersect with the skeleton of the ABS template. The log-likelihood $P(x|w_1)$ of class w_1 (contamination) and the log-likelihood $P(x|w_2)$ of class w_2 (non-contamination) are plotted in Figure 5.

E. Angle measurement

For case 3, the angle between two cross-points relative to the circle center is calculated.

$$angle = cos^{-1}\left(\frac{AC \cdot BC}{|AC||BC|}\right) \quad (1)$$

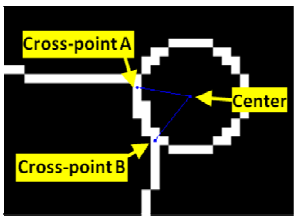

Contamination circle, angle = 60.8 degrees

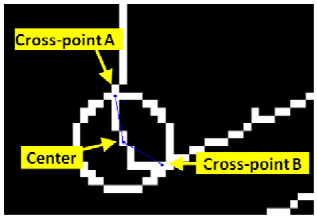

Non-contamination circle, angle = 130.4 degrees

Figure 6. Example of detected circles; a)-b) contamination circles, (c) non-contamination circle.

where A and B are the two cross-points and C is the center of the detected circle. The line between the cross-points A and C is denoted AC, and the line between the cross-points B and C is denoted BC. If there are more than two cross-points, more than one angle is calculated and the largest angle is selected [5]. Example of angles between two cross points and the circle center are shown in Figure 6.

F. Decision making

Finally, the algorithm makes a decision whether the detected circle represents a contamination or not. For case 1 and case 2 the likelihood of each case is used to classify the detected circle into one of the two classes, namely the contamination class w_1 or the non-contamination class w_2. From Bayesians theory one know that $P(w_i|x)$ varies directly as the $P(x|w_i)$.

$$P(w_i|x) \ \alpha \ P(x|w_i) \quad (2)$$

If $P(w_1|x)$ is greater than $P(w_2|x)$, the detected circle is considered contaminated.

$$x \in w_1 \ \ if \ \ P(x|w_1) > P(x|w_2) \quad (3)$$

To employ the prior probability $P(w_i)$, $P(w_i|x)$ are obtained from;

$$P(w_i|x) = \frac{P(w_i|x)P(w_i)}{P(w_1|x)P(w_1) + P(w_2|x)P(w_2)} \quad (4)$$

where $i = [1, 2]$ for the contamination and non-contamination classes, respectively.

In Eq.(4), $P(w_1)$ and $P(w_2)$ are prior probabilities of class w_1 contamination and class w_2 non-contamination which are computed from the location of the contamination circles and non-contamination circles detected from the images in the

training set. The skeleton of the ABS template image is divided into 12 equal sub-regions and the detected circles are traced on the skeleton of each region. Then we count the number of circles that cross the skeleton. For each sub-region, the prior probabilities value $P(w_1)$ is computed from the number of circles from class w_1, and $P(w_2)$ is computed from the number of circles from class w_2.

For case 3, if the angle is less than a threshold (90 degrees) the circle area is considered a contamination. For circles with angles greater than the threshold, the likelihood according to (3), and the prior probability according to (4) are used to make a decision about whether the potential contamination area is contaminated.

IV. Experimental Evaluation

The proposed method was tested with 1,363 HGA images. The test images were acquired by a mechanical positioning tool that positioned the camera to take the pictures. This test suite comprised 1,050 images without contaminations, 500 images of these non-contamination images were used to calculate the likelihood and the prior probability, and 313 images with contaminations which were used to calculated the likelihood and the prior probability. The results were compared to those reported in [5] where angle measurement and intensity were used to identify contamination in ABS images. We also report the results when 1) the proposed method used the likelihood, the prior probability and angle measurement without template registration, 2) the proposed method used only the likelihood without template registration, and 3) the proposed method used the likelihood and angle detection method with template registration. The methods were implemented in Matlab and run on a Windows PC. The results are shown in Table I. False detections in non-contamination images are denoted "over reject", and false detections in contamination image are denoted "under reject".

The previous method yields an over reject rate of 17.8% and an under reject rate of 26.8%. The method proposed herein without template registration yields an over reject rate of 10.7% and an under reject rate of 25.2%. The proposed algorithm with likelihood estimation and template registration gives an over reject rate of 21.7 % and an under reject rate of 8.6%. Finally, by fusion the proposed likelihood and angle detection method with template registration an over reject rate of 12.6% and an under reject rate of 10.5% is achieved.

To evaluate the performance of the methods, the following performance evaluation measurements were used [15], namely sensitivity, specificity, precision, and accuracy. The results are shown in Table II.

The proposed combined method achieves a sensitivity of 87.4%, a specificity of 89.5%, a precision of 96.5% and an accuracy of 87.9%, while the previous method only provided a sensitivity of 82.2%, specificity of 73.2%, precision of 91.1% and an accuracy of 80.1%. In hard disk drive manufacturing, the sensitivity and specification important indicators. The algorithm that employs likelihood estimation without template registration provides the highest overall specificity of 91.4%, while the sensitivity is low with a rate of only 78.3%

TABLE I. Experimental Results

Method	Over Reject, %	Under Reject, %
Previous method	187, 17.8%	84, 26.8%
Likelihood, prior, angle measurement without template registration	112, 10.7%	79, 25.2%
Likelihood without template registration	228, 21.7%	27, 8.6%
Fusion of likelihood and angle detection method with template registration	132, 12.6%	33, 10.5%

TABLE II. Performance Evaluation

Method	Sensitivity	Specificity	Precision	Accuracy
Previous method	82.2%	73.2%	91.1%	80.1%
Likelihood, prior, angle measurement without template registration	89.3%	74.8%	92.2%	86.%
Likelihood without template registration	78.3%	91.4%	96.8%	81.3%
Fusion of likelihood and angle detection method with template registration	87.4%	**89.5%**	96.5%	**87.9%**

V. Conclusions

This paper proposes the fusion of maximum likelihood and angle features to detect micro-contamination on the ABS of the hard disk drive head gimbal assembly. Experimental results validated the improvement of the proposed method compared to the previous method.

Acknowledgements

This project was financially supported by the Thailand Research Fund (TRF).

References

[1] Z. S. Chow, M. Po-Leen Ooi, Y. C. Kuang, S. Demidenko, "Low-cost automatic visual inspection system for media in hard disk drive mass production," Instrumentation and Measurement Technol Conf (I2MTC), pp. 234-239, 2012.

[2] Z. S. Chow, M. Po-Leen Ooi, Y. C. Kuang, S. Demidenko, "Automated visual inspection system for mass production of hard disk drive media," Elsevier, Procedia Engineering, vol 41, pp. 450-457, 2012.

[3] W. Withayachumnankul, P. Kunakornvong, C. Asavathongkul, and P. Sooraksa, "Rapid detection of hairline cracks on the surface of piezoelectric ceramics," Int. J. Adv. Manuf. Technol., vol. 64, Issue: 9-12, pp.1275–1283, Feb. 2013.

[4] S. Yammen, and P. Muneesawang, "An advanced vision system for the automatic inspection of corrosions on Pole Tips in hard disk drives," IEEE Trans. Compon. Packag. Manuf. Technol., pp. 1-11, Jul. 2014.

[5] J. Ieamsaard, P. Muneesawang, and F. E. Sandnes. "Image based contamination detection on hard disk head gimbal assembly," In 2015 11th International Conference on Signal-Image Technology & Internet-Based Systems (SITIS), pp. 143-146, 2015.

[6] P. Liang, X. Zhiwei, and D. Jiguang, "Fast normalized cross-correlation image matching based on multiscale edge information," Proceeding of International Conference on Computer Application and System Modeling (ICCASM), pp. 507-511, 2010.

[7] S. Klein, M. Staring, K. Murphy, M. A. Viergever, and J.P. Pluim. "Elastix: a toolbox for intensity-based medical image registration," Medical Imaging, IEEE Transactions on 29, no. 1, pp.196-205, 2010.

[8] R. Fattal. "Image upsampling via imposed edge statistics," In ACM Transactions on Graphics (TOG), vol. 26, no. 3, pp. 95, 2007.

[9] T. Nodes, , and G. Jr. Neal "Median filters: some modifications and their properties," IEEE Transactions on Acoustics Speech and Signal Processing, pp. 739-746, 1982.

[10] P. Muneesawang, N. Zhang, and L. Guan, "Image Retrieval from a Forensic Cartridge Case Database," In Multimedia Database Retrieval Springer International Publishing, pp. 147-167, 2014.

[11] N. Otsu, "A threshold selection method from gray-level histograms," Automatica 11, no. 285-296, pp. 23-27, 1975.

[12] D. Barker, "Seeing the wood for the trees: philosophical aspects of classical, Bayesian and likelihood approaches in statistical inference and some implications for phylogenetic analysis," , Biology & Philosophy 30, no. 4, pp. 505-525, 2015.

[13] B.U. Park, S. Léopold, and Z. Valentin, "Categorical data in local maximum likelihood: theory and applications to productivity analysis,", Journal of Productivity Analysis 43, no. 2, pp. 199-214, 2015

[14] P.S. Sisodia, V. Tiwari, and A. Kumar, "Analysis of supervised maximum likelihood classification for remote sensing image,", InRecent Advances and Innovations in Engineering (ICRAIE), 2014, pp. 1-4. IEEE, 2014.

[15] J. Han and M. Kamber, Data mining: concepts and techniques, San Francisco, CA, USA: Morgan Kaufmann, 2006, ch. 6.

[16] R. O. Duda, P. E. Hart, D. G. Stork, Pattern classification, John Wiley & Sons, 2012.